Mechanical phase diagram of shrinking cylindrical gels

Arezki Boudaoud[1] and Sahraoui Chaïeb[2,3]

[1]*Laboratoire de Physique Statistique de l'ENS, 24 rue Lhomond, 75231 Paris Cedex 05, France*
[2]*Theoretical and Applied Mechanics, University of Illinois at Urbana-Champaign, 104 South Wright Street, Urbana, Illinois 61801, USA*
[3]*The Beckman Institute for Advanced Science and Technology, 405 North Mathews Avenue, Urbana, Illinois 61801, USA*

When polymer gels are subjected to an external stimulus such as temperature or solvent change, they undergo a phase transition often driving pattern formation. In this paper, we use an elastic model to investigate the linear stability of shrinking cylindrical NIPA gels. This model exhibits bubble and bamboo patterns. The wavelengths of these patterns and their phase diagram are in agreement with the experiment of Matsuo and Tanaka [Nature (London) **358**, 482 (1992)].

I. INTRODUCTION

Gels exhibit many fascinating patterns [1]. Natural gels are found in animal tissues and plant bodies, while synthetic gels are used in manufacturing devices such as actuators and valves; and in biomedical applications such as molecular sieves. Almost all artificial organs are tissue-engineered by seeding cells in a three-dimensional scaffold made of a biocompatible polymeric gel [2]. Polymeric hydrogels are a mixture of a polymeric network and water. Because polymeric hydrogels exhibit many metastable phases and strong hysteresis during phase changes, they are considered to be ideal models for the folding of proteins, which have a complex set of metastable states [3–5]. When submitted to external stimuli such as variations in temperature, pH, osmotic pressure [6,7], electric field [8] or light [9], polymeric hydrogels undergo huge volume changes. These properties are useful for technological applications, such as actuators in microfluidic devices [10,11], where the volume change can be used to actuate the device. During these phase transformations involving shrinking and swelling, patterns driven by different instabilities are observed and are not yet completely understood. Pattern formation in gels and their kinetics have been first studied by Tanaka and co-workers [1,12–14]. Many experimental [15–20], numerical [21–23], or analytical [24–30] studies have followed. These patterns not only represent a challenging problem in physics and mechanics but also might shed light on the mechanical behavior of animal tissue. For instance, the swelling of a gel is similar to the growth of a tissue, and the folding of the brain might result from growth induced stresses as the folding of a spherical gel results from swelling induced stresses. Shrinking cylindrical gels (such as those in Fig. 1) are also morphologically similar to some deep-sea organisms or plants [31]. Understanding the mechanism of gel shrinking could lead to a better understanding of plant and human skin wrinkling as they dry.

In this paper we study the shrinking of cylindrical gels and the resulting patterns, first investigated by Sato-Matsuo and Tanaka [14]. Sato-Matsuo and Tanaka studied the shrinking of cylindrical hydrogels immersed in acetone where they undergo a shrinking transition. Mainly bubble and bamboo patterns were observed (Figs. 1 and 2). The bubble pattern looks like the Rayleigh instability known in hydrodynamics

or a peristaltic instability observed in vesicles [32,33]: The cylindrical shape was lost and alternate shrunken (constrictions) and swollen (bulges) regions appeared. In the bamboo pattern, the gel remained cylindrical while regularly spaced cross-sectional planes consisting of collapsed gel appeared; these planes were believed to be fractures [34]. Previous theoretical studies [29,30] have predicted bubbles only. Here we recall and mimic the experimental observations and we provide a comprehensive theoretical study of the shrinking patterns. The paper is organized as follows. In Sec. II, we give our experimental observations, following [14]. In Sec. III, we describe a simple model coupling the interactions between the polymer and the solvent to the elasticity of the polymer network. We investigate the linear stability of a cylindrical gel and we derive a phase diagram and compare it with the experimental diagram reported by Sato-Matsuo and Tanaka [14].

II. EXPERIMENTAL OBSERVATIONS

Following Sato-Matsuo and Tanaka [14], we prepared cylindrical acrylamide gels of various diameters by bulk polymerization of a polymer. The monomer used for the polymerization is *N*-isopropylacrylamide (*N*-IPA), *N*,*N*'-methylenebisacrylamide (BIS) is the crosslinker, ammonium persulfate (APS) is the initiator, and tetramethylethylenediamine (TEMED) is the accelerator. We used sodium acrylate to change the ionic strength of the gel. All these
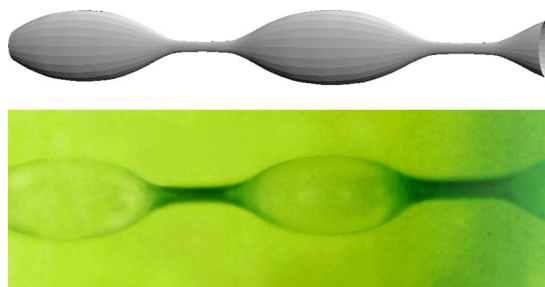

FIG. 1. The bubbles pattern of a shrinking cylindrical gel. The top is the theoretical illustration given by Eqs. (6) and (7) to the bottom experimental picture. The picture in the bottom is from Sato-Matsuo and Tanaka [14].
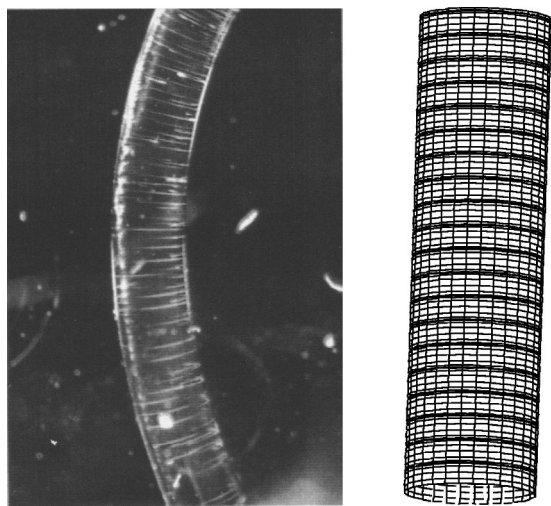
FIG. 2. Bamboo pattern for a shrinking cylindrical gel. Left: experimental observations. Right: corresponding theoretical shapes from the eigenmodes given by Eqs. (6) and (7). The gel remains cylindrical and is crossed by regularly collapsed planes.

chemicals were purchased from Polysciences. The gel was prepared in glass tubes with varying diameter from 0.5 mm to 2 mm, so that cylindrical gels were obtained. Various methods were used to extract the gels from the tubes. The easiest method consisted in putting the tubes in a water solution and letting the inner gel swell. The swollen gels have a tendency to slip out of the tubes. This extrusion process was expedited by suspending the glass tube vertically and letting the inner gel slide out by gravity and fall in the water container to be washed from the remaining chemicals.

After drying, the ends of the cylinder were either left free or glued to glass rods to control their separation. The cylindrical gels were allowed to swell in water and, after they reached equilibrium, they were placed in an acetone-water mixture, so that they shrank. The final state of the gel depended on the volume change, the acetone content of the mixture and (if relevant) the separation of the glass rods. Different cases were observed.

(1) Stable cylinder. The cylindrical gel shrinks homogeneously and remains cylindrical.

(2) Bubble pattern (Fig. 1). The cylindrical shape is lost and alternate shrunken and swollen regions appear, with a well-defined wavelength. The wavelength is proportional to the cylinder radius: $\lambda \sim R$.

(3) Bamboo pattern (Fig. 2). The gel remains cylindrical and regularly spaced cross sections formed of collapsed gel are observed. Their thickness is of the order of 1 μm, as interference pattern observed in these cross-sectional planes in Ref. [14] suggest that the thickness of these planes is of the order of magnitude of the wavelength of light. The wavelength of the pattern is also well defined and is proportional to the square root of the radius: $\lambda \sim \sqrt{R}$.

(4) Bamboo-in-bubble. The two previous patterns occur sometimes at the same time. The cylindrical shape is lost and collapsed cross sections appear. Within every bubble cross-sectional planes are observed suggesting a bamboo pattern.

(5) Wrinkled tubes. The gel becomes opaque and its sur-

face wrinkled at a scale much smaller than the radius. The inner portion of the gel consists of collapsed and swollen regions, in the shape of concentric thin sheets, which can be peeled off easily. The pattern is quite irregular.

A. Shrinking of gels with free ends

We now discuss the particular case when the gel ends are free. The final state depends mainly on the acetone content. It was found in Ref. [14], that the varieties of patterns, which appear as the concentration of acetone is changed, are quite different between plain and Dextran containing gels. Plain gels predominantly form bamboos, while Dextran gels form bubbles. Dextran is a water soluble polymer used in the study by Sato-Matsuo and Tanaka [14] to color the cylinders in blue for easy observation. (The cylinders are transparent and shrunken regions are hard to see when the concentration of cross linker is small.) It was found, however, that Dextran affects the phase diagram of the shrinking gels. This effect is beyond the scope of this paper and we will not discuss it any further.

In Dextran-free gels or plain gels, the bamboo pattern appears between 40% and 70% in acetone concentration. At 80% of acetone concentration, the spacing between cross-sectional planes becomes narrower. The onset of pattern formation occurs earlier in time at higher concentration of acetone. Wrinkled tubes are observed at concentrations of acetone from 90% to 100%. Their irregularity increases with the acetone content.

In Dextran gels, bubbles appear from 40% to 80% acetone concentration. The wavelength increases as acetone concentration increases.

The wavelength and onset of the instability depend on the size of the cylinder. However, from the moment when the pattern appears, it takes a long period of time to reach the final equilibrium state. The process seems to be governed by diffusion, since the characteristic times scale as the square of the radius of the tube [14].

B. Shrinking with fixed final length

The final length of the gels is now controlled by the separation of the glass rods to which the cylinder ends are glued. The state of the gel depends on the acetone content and the final length of the gel. (See Fig. 5 for an experimental phase diagram.) Mainly bubbles and bamboos are observed: bubbles occur at large separations or small acetone content (typically smaller than 60%); mixed bamboo in bubbles can be observed near the limit between the bubbles and bamboos. At very high acetone concentration, wrinkled tubes are observed. As in Ref. [14], we also used sodium acrylate to change the ionic strength. At higher ionic strength, bamboos are observed only at larger acetone content.

When increasing acetone concentration, the bubbles wavelength increases, while the bamboos wavelength decreases. The wavelengths of both patterns increase as the fixed final length is increased. We have also observed that the wavelength increases with increasing ionic content by increasing the concentration of sodium acrylate in the gel.

III. THE THEORY

A. Model

We first describe a simple model accounting for the interaction between the polymer and the solvent, the deformations of the network and its density correlations. We consider the polymer volume fraction ϕ to be ϕ_0 in the reference state (the state where the network was first polymerized). The free energy of the gel is the sum of three terms,

$$\beta G = E_{int} + E_{el} + E_{corr}. \tag{1}$$

Here $1/\beta = k_B T$ is the energy unit.

The first term accounts for the interaction between the polymer and the solvent, and for the isotropic part of the elastic energy [35]. It is given by an integral over the volume of the gel

$$E_{int} = \int d\mathbf{r} f(\phi). \tag{2}$$

The shape of $f(\phi)$ determines the number and the stability of the different possible phases. It may depend on the external parameters, such as the composition of the solvent (in our case it would be the acetone content). If $f(\phi)$ has one minimum then only one phase with density ϕ_0 exists. If $f(\phi)$ has two minima, then two stable phases exist (one of them is possibly metastable), and one unstable phase; this is usually the case in poor solvent conditions. At this stage of the analysis, we will not specify the specific form of f. We will do so when we compare our theortical results with the experimental results. In the rest of the calculation, we will only use the value of its second derivative at the considered equilibrium density $f''(\phi_s)$, so that the theoretical results for the linear stability analysis are generic and hold for both swelling and shrinking (see following subsection). If $f''(\phi_s) > 0$, then the density ϕ_s corresponds to a stable phase, whereas if $f''(\phi_s) < 0$, this equilibrium is unstable, and a spinodal decomposition is expected.

If the position of a volume element $\mathbf{r}$ is displaced from its reference position $\mathbf{r}^\circ$ in the reference state, then the deformation of the network is described by the deformation matrix $M_{ij} = \partial r_i / \partial r_j^\circ$. M and the density ϕ are not independent but they are related via $\phi_0/\phi = \det M$. The anisotropic part of the elastic energy indicates the cost due to shear deformations. It is a function of the deformation matrix M in terms of its invariants. The form that is consistent with the Flory microscopic description [23,36] is

$$E_{el} = \frac{1}{2} \int d\mathbf{r} \, \mu \, \mathrm{Tr}(M^t M). \tag{3}$$

Here $\mu = \mu_0 \phi / \phi_0$ is the effective chain density per unit volume (alternatively the cross-links density), μ_0 being its value in the reference state.

The last term in the free energy has the Ornstein-Zernicke form [36,37] and accounts for the density correlations in the gel,
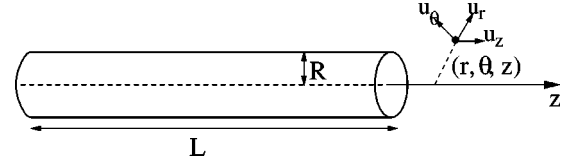

FIG. 3. Geometry of the model.

$$E_{corr} = \frac{1}{2} \int d\mathbf{r} \frac{1}{2} K(\phi) |\nabla \phi|^2. \tag{4}$$

$l = \sqrt{K/\mu}$ is of the order of the correlation length of density fluctuations in the gel.

The Lagrangian gel evolution equation [38] reads

$$g \frac{\partial \mathbf{r}}{\partial t} = -\beta \frac{\delta G}{\delta \mathbf{r}}, \tag{5}$$

$g/\beta \equiv f \sim 10^{17}$ N s/m^4 is the gel-solvent friction coefficient [39]. We neglect the inertia of the gel as g is very large and we implicitly assume that the solvent is at rest.

B. Basic state and linear stability analysis

We consider a cylindrical gel of radius R_0 and length L_0 as a reference state (the state where the gel was polymerized, Fig. 3). The gel is placed in an acetone-water mixture so that it is submitted to an osmotic pressure π. It shrinks to an unknown radius R while its length is constrained to be L. The gel elongation ratios are $\alpha_r = R/R_0$ and $\alpha_z = L/L_0$. The polymer volume fraction becomes $\phi_s = \phi_0/(\alpha_r^2 \alpha_z)$. The gel equilibrium state is determined by $\delta(G + \pi V) = 0$,

$$\beta \pi = \phi_s f'(\phi_s) - f(\phi_s) - \mu \alpha_r^2. \tag{6}$$

To summarize, the equilibrium basic state is a uniformly deformed cylinder with elongations α_r and α_z such that Eq. (6) is satisfied.

The next step is to study the linear stability of this basic state. We use cylindrical coordinates r, θ, z (Fig. 3). The reference position vector $\mathbf{r}^\circ = r\mathbf{u}_r + z\mathbf{u}_z$ has been displaced to $\mathbf{r}_s = \alpha_r r\mathbf{u}_r + \alpha_z z\mathbf{u}_z$. We consider perturbations to this uniformly elongated state such that $\mathbf{u} = \mathbf{r} - \mathbf{r}_s = u_r\mathbf{u}_r + u_z\mathbf{u}_z$ is small. The dynamical equation for $\mathbf{u}$ is derived from Eq. (5):

$$g \frac{\partial u_r}{\partial t} = \tau \frac{\partial}{\partial r} \nabla \cdot \mathbf{u} + \mu \alpha_z^2 \frac{\partial^2 u_r}{\partial z^2} + \mu \alpha_r^2 \frac{\partial}{\partial r} \nabla_r u_r - \kappa \frac{\partial}{\partial r} \Delta \nabla \cdot \mathbf{u}, \tag{7}$$

$$g \frac{\partial u_z}{\partial t} = \tau \frac{\partial}{\partial z} \nabla \cdot \mathbf{u} + \mu \alpha_z^2 \frac{\partial^2 u_z}{\partial z^2} + \mu \alpha_r^2 \Delta_r u_z - \kappa \frac{\partial}{\partial z} \Delta \nabla \cdot \mathbf{u}. \tag{8}$$

Here $\nabla_r = \nabla \cdot - \partial/\partial z$, $\Delta = \nabla^2$, and $\Delta_r = \Delta - \partial^2/\partial z^2$; $\tau = \phi_s^2 f''(\phi_s)$ and $\kappa = K(\phi_s)$.

As stated earlier, the equations do not depend on the shape of the interaction function $f(\phi)$ but only on its second derivative at the equilibrium density $f''(\phi_s)$. In the case were the network does not resist shear ($\mu = 0$) and if $\tau < 0$, one recognizes in Eqs. (7) and (8) the standard equations used for

the description of the early stages of a spinodal decomposition. The free energy used here can be viewed as a model for spinodal decomposition for a system resisting shear.

We look for solutions of Eqs. (7) and (8) with growth rate σ/g and axial wave number k, i.e., $\mathbf{u} = \mathbf{v}\exp[(\sigma/g)t + ikz]$. Some calculations lead to the expressions

$$v_r = i[-aq_1I_1(q_1r) - bq_2I_1(q_2r) + ckI_1(q_3r)], \quad (9)$$

$$v_z = akI_0(q_1r) + bkI_0(q_2r) - cq_3I_0(q_3r). \quad (10)$$

I_0 and I_1 are modified Bessel functions. The radial wave numbers q_1 and q_2 are the positive solutions of

$$\sigma = -\tau(k^2-q^2) - \mu\alpha_z^2k^2 + \mu\alpha_r^2q^2 - \kappa(k^2-q^2)^2, \quad (11)$$

while the last wave number q_3 is the positive solution of

$$\sigma = -\mu\alpha_z^2k^2 + \mu\alpha_r^2q^2. \quad (12)$$

a, b, and c are complex constants.

These eigenvectors should satisfy the boundary conditions at $r = R$. The first two correspond to the vanishing of the stress tensor at the outer boundary. In other words,

$$(\tau - \mu\alpha_r^2)\nabla\cdot\mathbf{u} + 2\mu\alpha_r^2\frac{\partial u_r}{\partial r} - \kappa\Delta\nabla\cdot\mathbf{u} = 0, \quad (13)$$

$$\alpha_r^2\frac{\partial u_r}{\partial r} + \alpha_z^2\frac{\partial u_r}{\partial z} = 0. \quad (14)$$

The last one fixes the position of the interface between the gel and the solvent

$$\frac{\partial}{\partial r}\nabla\cdot\mathbf{u} = 0. \quad (15)$$

Mathematically, this condition insures the vanishing of the surface integral corresponding to the density correlation term in the energy.

The state of the gel is defined by three numbers: the ratio of elongations $\alpha = \alpha_r/\alpha_z$, the reduced second derivative of f, $\tilde{\tau} = \tau/(\mu\alpha_r^2)$, and the reduced correlation length $\tilde{\kappa} = \kappa k^2/(\mu\alpha_r^2)$. The boundary conditions give a solvability condition that determines the growth rate $\sigma = \sigma(\alpha, \tilde{\tau}, \tilde{\kappa}, kR)$,

$$H\left(\frac{q_1}{k}, \frac{q_2}{k}, \frac{q_3}{k}, kR, \alpha, \tilde{\kappa}\right) = H\left(\frac{q_2}{k}, \frac{q_1}{k}, \frac{q_3}{k}, kR, \alpha, \tilde{\kappa}\right), \quad (16)$$

where

$$H(\beta_1, \beta_2, \beta_3, \rho, \alpha, \tilde{\kappa}) = \beta_1^2(1-\beta_1^2)\{[\beta_3^2 + 1 + \beta_2^2(1-\beta_2^2)\tilde{\kappa}]$$
$$\times(\beta_3^2 + \alpha^2)\Psi(\beta_2\rho)$$
$$- 2\beta_2^2(1+\alpha^2)\Psi(\beta_3\rho)$$
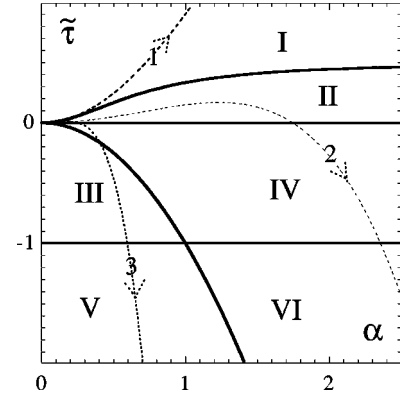$$+ \beta_2^2(1-\beta_3^2)\}. \quad (17)$$

FIG. 4. The general phase diagram: the different possible behaviors of the gel as a function of the elongations ratio $\alpha = \alpha_z/\alpha_r$ and the reduced second derivative of the isotropic part of the energy density f, $\tilde{\tau} = \alpha_z\phi_s^2 f''(\phi_s)/\mu_0$. I, stable gel; II, bubble; III, bamboo; IV, surface spinodal decomposition; V, skin formation; VI, radial spinodal decomposition. The dotted curves show the three possible paths followed by the system when reaching equilibrium: stable (1), bubble (2), bamboo (3).

The function Ψ is defined by $\Psi(\rho) = I_1(\rho)/I_0(\rho)$. The reduced growth rate σ reaches it maximum for $k = k_m$; if this maximum is positive then the cylindrical gel is unstable and the selected pattern is given by the eigenmode with axial wave number k_m. The study of the most unstable mode gives the phase diagram of Fig. 4. To obtain this diagram we have used the fact that the correlation length $l = \sqrt{\kappa/\mu}$ is small ($l \ll R$).

The diagram is split into six regions corresponding to different patterns (Fig. 4).

(I) Stable cylinder. The cylindrical gel is stable only in this first region.

(II) Bubble. In this region the most unstable mode has an axial wave number

$$k_m = K(\alpha, \tilde{\tau})/R \quad (18)$$

(K is a nondimensional function) and a radial wave number $q_m \sim R$. As $u_r(R) \neq 0$, the surface of the gel is periodically deformed, so that this region corresponds to the bubble pattern (see Fig. 1). Its wavelength is proportional to the gel radius as in the experiment. A simple interpretation for this instability comes from the fact that the elastic energy favors isotropic deformations: one expects the gel to be unstable if it is strongly stretched in one direction.

(III) Bamboo. In this region, the most unstable wave number is

$$k_m = \sqrt[4]{\mu(\alpha_r^2 - \alpha_z^2)/\kappa}\sqrt{z_0/R}. \quad (19)$$

z_0 is the first root of the Bessel function J_0. The corresponding radial wave number is $q_m \sim 1/R$. As $u_r(R) \simeq 0$, the gel remains cylindrical; it is periodically collapsed along its axis, so this region corresponds to the bamboo pattern (see Fig. 2). The wavelength is proportional to $\sqrt{R}$ and increases with the axial elongations as in the experiment. In this region, as well as in the following regions (IV–VI), a gel that does not resist

shear would undergo spinodal decomposition ($\tau<0$), so that we expect short wavelength instabilities.

(IV) Surface spinodal decomposition. In this region, the wave numbers are large, $k_m \sim q_m \sim \sqrt{\mu/\kappa}=1/l$ and spinodal decomposition occurs on the surface, which is expected to become rough.

(V) Skin formation. In this region, the wave numbers are $k_m=0$ and $q_m \sim 1/l$. The deformations are also localized on the surface. Surface shrinking is expected.

(VI) Radial spinodal decomposition. In this region, the wave numbers are $k_m=0$ and $q_m \sim i/l$. Spinodal decomposition occurs in the radial direction.

Regions (I–III) compare well with the experiment. The bubble pattern is an elastic instability resulting from a strongly anisotropic elongation. The bamboo pattern is a spinodal decomposition of a shear resisting material in a confined geometry. Regions (IV–VI) have a less obvious interpretation as they only have microscopic features. Wrinkled tubes are likely to originate from a mixture of regions (IV) and (VI): their surface is rough (as in region IV) and their inner regions consist of thin sheets, which can be peeled off. (This suggests a radial spinodal decomposition as in region VI.) These results show that the minimal model we use is sufficient to predict the main observed instabilities in shrinking gels.

C. Comparison with the experimental phase diagram

To translate this general diagram in experimental terms and compare it to Matsuo and Tanaka's results [14], we need to specify the form of the isotropic energy density $f(\phi)$. To simplify, we assume that acetone-water ratio is the same inside and outside the gel. If ϕ is the polymer volume fraction in the gel and x the acetone volume fraction in the solvent, then $(1-x)(1-\phi)$ and $x(1-\phi)$ are, respectively, the water and acetone volume fraction in the gel. The natural extension of the Flory energy [35] is then

$$f(\phi) = \frac{N}{v_w}[(1-x)(1-\phi)\ln(1-x)(1-\phi)$$

$$+ \chi_w(1-x)(1-\phi)\phi] + \frac{N}{v_a}[x(1-\phi)\ln x(1-\phi)$$

$$+ \chi_a x(1-\phi)\phi] + \frac{\mu_0}{2}\frac{\phi}{\phi_0}\left(\ln\frac{\phi}{\phi_0} - 3\right). \quad (20)$$

Here N is the Avogadro number, v_w and v_a are the water and acetone molar volumes, χ_w and χ_a are the polymer water and acetone-water interaction parameters. In the case of no acetone, this form of $f(\phi)$ fits well the experimental temperature to swelling ratio curve of NIPA gels: Hirotsu *et al.* [40] found $\phi_0=0.07$, $\mu_0=1.2\times10^{27}$ m^{-3} (we use these two values in the following), $\chi_w=-16.5$ at 20°C and $\chi_w=18$ at 35°C. These values, however, are not in agreement with independent estimations as noticed in Ref. [40]. In Ref. [14], spinodal decomposition does not occur when water is used as solvent but occurs when acetone is used as a solvent; so, we
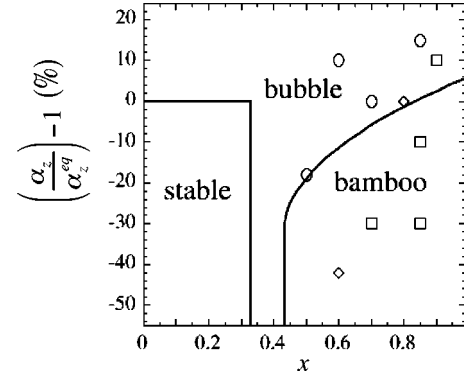

FIG. 5. The phase diagram: the axial elongation α_z (normalized by its value α_z^{eq} at equilibrium in water) as a function of the acetone volume fraction x in the solvent. Continuous lines: theory using a criterion based on the different paths in Fig. 4. Symbols, experiment of Matsuo and Tanaka [14]; squares, bamboo patterns; circles, bubble patterns; diamonds, mixed bamboo-in-bubble.

use the reasonable values $\chi_w=0$ and $\chi_a=10$. The following results are only slightly sensitive to these values.

The phase diagram we have obtained is valid when the gel is at equilibrium with the solvent, whereas in Ref. [14], the pattern develop before equilibrium is reached and while the solvent is still diffusing out of the gel. Even if the gel is not in equilibrium, the linear stability analysis should give good indications on the possible patterns. Besides, we consider that before the onset of the instability, the density is uniform in the gel. This assumption might seem too strong because the gel shrinks through a diffusive process and a collapsed skin forms at its periphery. In fact, our assumption means that we replace the non uniform density by a uniform density such that the two densities (uniform and non uniform) have the same mean. The existence of a small zone with a different density (the skin) should not affect the mean.

We consider that the volume fraction $\phi=\phi_0\alpha^2/\alpha_z^3$ is uniform in the gel but is a non decreasing function of time (the gel shrinks). Then in the diagram of Fig. 4, the gel follows a path $\tilde{\tau}(\alpha)=\alpha_z f(\phi_0\alpha^2/\alpha_z^3)/\mu_0$. Figure 4 shows the three possible path types: The first path remains in zone I, so we expect the tube to remain stable; the second spans a long period of time in zone II, so we expect bubbles to be observed; the third path spends a little time in zones II and IV then passes to zone III, so we expect bamboo patterns. Each path is only determined by the values of the experimental parameters α_z and x. Using the form of $f(\phi)$ [Eq. (20)], we related τ to the acetone content and we computed the limits between the path types in the (x, α_z) parameters plane. Thus we obtained the phase diagram of Fig. 5. As our criterion is rough, the limits between the phases are not well defined. However, this diagram is in quantitative agreement with the experimental results of Ref. [14]. Moreover, we could extend our results to ionized gels by multiplying the last term of Eq. (20) by $(1+2I)$, I being the number of counterions per effective chain [35]. In this case, the diagram is shifted towards higher acetone concentration as in the experiment [14].

We can compute the typical time scale for the growth of the patterns, $T=g/\sigma \sim g/(\mu q_m^2)$. Given the aforementioned

values and for a gel of radius 1 mm, the time scale is found to be 10 min. It is of the same order of magnitude as in the experiments.

IV. CONCLUSION

Using a simple elastic model and an extension of the Flory free energy of gels, the experimental results on the patterns arising when cylindrical gels shrink were reproduced theoretically: the wavelengths of the bamboo and the bubbles instabilities first observed by Sato-Matsuo and Tanaka were computed and the phase diagram observed experimentally was reproduced with quantitative agreement.As an extension to this work, we are investigating pattern formation when a gel membrane undergoes a shrinking transition [41]. These preliminary results showed patterns similar to the crumpling of elastic sheets [42,43]. We expect this type of modeling to give insights in gel deformations and buckling of ''soft'' materials and to be useful for bioengineering applications and manufacturing such as small robots and biomedical devices and actuators [11].

[1] T. Tanaka *et al.*, Nature (London) **325**, 796 (1987).

[2] R.S. Langer and J.P. Vacanti, Science **260**, 920 (1993); R.S. Langer and J.P. Vacanti, Sci. Am. **280**, 86 (1999).

[3] Y. Takeoka *et al.*, Phys. Rev. Lett. **82**, 4863 (1999).

[4] M. Annaka, M. Tokita, T. Tanaka, S. Tanaka, and T. Nakahira, J. Chem. Phys. **112**, 471 (2000).

[5] T. Enoki *et al.*, Phys. Rev. Lett. **85**, 5000 (2000).

[6] T. Tanaka, Phys. Rev. A **17**, 763 (1978).

[7] T. Tanaka *et al.*, Phys. Rev. Lett. **45**, 1636 (1980).

[8] T. Tanaka, I. Nishio, S.-T. Sun, and S. Ueno-Nishio, Science **218**, 467 (1982).

[9] S. Juodkazis *et al.*, Nature (London) **408**, 178 (2000).

[10] Z. Hu, X. Zhang, and Y. Li, Science **269**, 525 (1995).

[11] D.J. Beebe *et al.*, Proc. Natl. Acad. Sci. U.S.A. **97**, 13488 (2000); D.J. Beebe *et al.*, Nature (London) **404**, 588 (2000).

[12] T. Tanaka, Physica A **140**, 261 (1986).

[13] E.S. Matsuo and T. Tanaka, J. Chem. Phys. **89**, 1695 (1988).

[14] E.S. Matsuo and T. Tanaka, Nature (London) **358**, 482 (1992).

[15] H. Tanaka, H. Tomita, A. Takasu, T. Hayashi, and T. Nishi, Phys. Rev. Lett. **68**, 2794 (1992).

[16] H. Tanaka and T. Sigehuzi, Phys. Rev. E **49**, R39 (1994).

[17] Y. Li, C. Li, and Z. Hu, J. Chem. Phys. **100**, 4637 (1994).

[18] S. Sasaki and H. Maeda, J. Colloid Interface Sci. **211**, 204 (1999).

[19] G. Bai and A. Suzuki, J. Chem. Phys. **111**, 10338 (1999).

[20] M. Tokita, K. Miyamoto, and T. Komai, J. Chem. Phys. **113**, 1647 (2000).

[21] T. Hwa and M. Kardar, Phys. Rev. Lett. **61**, 106 (1988).

[22] K. Sekimoto and K. Kawasaki, J. Phys. Soc. Jpn. **57**, 2594 (1988).

[23] N. Suematsu, K. Sekimoto, and K. Kawasaki, Phys. Rev. A **41**, 5751 (1990).

[24] K. Sekimoto and K. Kawasaki, J. Phys. Soc. Jpn. **56**, 2997 (1987).

[25] A. Onuki, J. Phys. Soc. Jpn. **57**, 703 (1988).

[26] K. Sekimoto and K. Kawasaki, Physica A **154**, 384 (1989).

[27] A. Onuki, Phys. Rev. A **39**, 5932 (1989).

[28] S. Panyukov and Y. Rabin, Macromolecules **29**, 8530 (1996).

[29] B. Barrière, K. Sekimoto, and L. Liebler, J. Chem. Phys. **105**, 1735 (1996).

[30] J.I. Maskawa, T. Takeuchi, K. Maki, K. Tsuji, and T. Tanaka, J. Chem. Phys. **110**, 10993 (1999). The no stress boundary conditions used here assume isotropy of the gel, which is not true when it is elongated.

[31] T.W. D'Arcy, *On Growth and Form* (Dover, New York, 1992).

[32] R. Bar-Ziv and E. Moses, Phys. Rev. Lett. **73**, 1392 (1994).

[33] S. Chaïeb and S. Rica, Phys. Rev. E **58**, 7733 (1998).

[34] P.-G. de Gennes, C. R. Acad. Sci., Ser. IIb: Mec., Phys., Chim., Astron. **324**, 343 (1997).

[35] P.J. Flory, *Principles of Polymer Chemistry* (Cornell University Press, Ithaca, NY, 1953).

[36] A. Onuki, J. Phys. Soc. Jpn. **57**, 699 (1988).

[37] P.-G. de Gennes, *Scaling Concepts in Polymer Physics* (Cornell University Press, Ithaca, NY, 1980).

[38] This not strictly speaking, an equation of motion but rather a Largangian formulation based on the free energy in Eq. (1).

[39] M. Tokita and T. Tanaka, J. Chem. Phys. **95**, 4613 (1991).

[40] S. Hirotsu, Y. Hirokawa, and T. Tanaka, J. Chem. Phys. **87**, 1392 (1987).

[41] S. Chaïeb and A. Boudaoud (unpublished).

[42] E. Cerda, S. Chaïeb, F. Melo, and L. Mahadevan, Nature (London) **401**, 46 (1999).

[43] A. Boudaoud, P. Patrício, Y. Couder, and M. Ben Amar, Nature (London) **407**, 718 (2000).